Available online at www.sciencedirect.com

ScienceDirect

Procedia CIRP 126 (2024) 692–697

www.elsevier.com/locate/procedia

17th CIRP Conference on Intelligent Computation in Manufacturing Engineering (CIRP ICME '23)

Surface characteristic of Ti-6Al-4V alloy fabricated by Electron Beam Melting prepared by different surface post treatments

Amir Behjat[a,b], Mohammad Hossein Mosallanejad[a], Morteza Shamanian[a], Aboozar Taherizadeh[a], Luca Iuliano[b], Abdollah Saboori[b,]*

[a] *Department of Materials Engineering, Isfahan University of Technology, 84156-83111 Isfahan, Iran*
[b] *Integerated Additive Manufacturing Center (IAM@Polito), Department of Management and Production engineering, Politecnico di Torino, Corso duca degli Abruzzi 24, 10129, Torino, Italy*

* Corresponding author. Tel.: +39-011-090-7285; *E-mail address:* Abdollah.saboori@polito.it

Abstract

Metal additive manufacturing (AM) is a technique in constant growth that offers freedom in design in the production of complex shape components. However, it is well documented that most types of material failures in the AM parts are very sensitive to their surface properties. Hence, in this work, some surface post-treatments such as grinding, drag finishing and Surface Mechanical Treatment (SMT) are used as post-treatment processes to improve the performance of Ti-6Al-4V samples fabricated by the Electron Beam Melting technique. The influences of different post-treatment were investigated on the surface properties. The outcomes demonstrated that the SMT has- the highest efficiency in the surface treatment and could reduce surface roughness, increase hardness and improve wettability. This work demonstrates the potential of SMT to achieve favourable surface properties of AM metallic components**.**

Peer-review under responsibility of the scientific committee of the 17th CIRP Conference on Intelligent Computation in Manufacturing Engineering (CIRP ICME'23)

Keywords: Metal Additive Manufacturing; Surface Mechanical Treatment; Ti-6Al-4V alloy; Electron Beam Melting; Microhardness; Wettability

1. Introduction

For many decades, metals and their alloys have been widely used in medical implants [1,2]. Compared to other metallic biomaterials, the low density, high specific strength, excellent corrosion resistance and high biocompatibility of titanium and its alloys make them widely used in clinical applications as the biomedical material [3,4]. However, titanium materials are well known as expensive and hard to process using traditional methods [5]. Additive manufacturing (AM) technology, known as the fourth industrial revolution, has become an attractive technology for manufacturing titanium-based alloys parts [6].

Electron beam melting (EBM), an emerging metal AM is considered as an innovative industrial production technology to produce medical implants and aviation components [2,7–9]. This technology uses a high energy electron beam as a heat source in the vacuum environment to fabricate alloy parts on a powder bed based on a computer aided designed (CAD) model [10,11]. It should be noted that a vacuum environment and pre-heat the powder feedstock before starting the EBM process led to producing a fully dense part of a series of important engineering alloys. Moreover, the high power of the electron beam led to a fast processing cycle and a high building rate [12]. Manufacturing parts by the EBM process allows the highest geometrical flexibility, accuracy, and defect-free components compared to the laser-based AM processes [13,14]. It is well reported that the EBM technique is suitable for the rapid production of medical implants based on the needs of each

Peer-review under responsibility of the scientific committee of the 17th CIRP Conference on Intelligent Computation in Manufacturing Engineering (CIRP ICME'23)
10.1016/j.procir.2024.08.289

individual patient [15]. Therefore, from the industrial perspective, EBM becomes a great alternative method for producing complex metal-based components, particularly those with complex shapes such as the porous Ti–6Al–4V (TC4) implants [16]. However, besides the aforementioned issues, it should be noted that the EBM process still has some disadvantages, such as high surface roughness and tensile residual stress near the surface layer [17,18]. These problems led to decreased corrosion resistance and mechanical properties of AM parts compared to conventionally manufactured ones. It should be noted that the surface roughness originating from the partially melted particles is one of the reasons for weak fatigue performance [9,19]. Therefore, post-processing of metal AM components is required to eliminate the superficial defects [18]. According to recent reports published by Wohler Report, Post-processing is one of three major phases of producing AM parts and nearly 27% of the production cost for the AM parts [20]. Recently, different post-treatment approaches such as thermal, mechanical and chemical methods were developed to improve the surface characteristics of the AM component [18]. According to previous studies, the post-treatment methods can be selected based on the application requirement, geometry complexity, size of parts and required surface quality [21]. Several studies have reported that (thermal or chemical) post processing enhances the surface quality and integrity of AM titanium (TC4) parts [19]. Hence, various mechanical surface treatments such as shot peening [22], vibratory finishing [23], tumbeling [24], ultrasonic shot peening (USSP) [25], laser peening (LP) [26], cavitation peening [9] and surface mechanical attrition treatment (SMAT) [27] are widely used to improved surface characteristics and mechanical properties of the AM metal component. Recently, Zhang et al. used ultrasonic nanocrystallization to modify the surface of AM TC4 parts and consequently enhance their fatigue performance. They found that, after ultrasonic peening, the surface roughness (*Ra*) can be reduced from 10.6 µm to 1.3 µm [28]. The efficiency of such a deformation-based SMAT process depends very much on the plasticity of the AM material [27]. Persenot et al. reported that even if the USP process can induce beneficial compressive stress, finer microstructure due to severe plastic deformation and low surface roughness of EBM TC4 parts, but many macroscopic subsurface residual defects will remain. The mechanism leading to formation of subsurface defects is folded protruding peaks of rough surface by mechanical surface post-treatment and creates a new surface which entraps the tip of the initial defects. They proposed that the benefits of USP as a mechanical post-treatment for metal AM parts could be further improved when combined with another post treatment to smooth surface irregularities before utilizing USP [29].

Despite lots of research that has been performed on the surface modification of the metal AM parts, far too little attention has been paid to the effect of various post-surface treatments of the surface characteristics of titanium parts fabricated by the EBM process. Hence, the main objective of this work is to investigate the effect of different surface post-treatment operations on the roughness, microhardness and wettability of the EBM Ti64 samples.

2. Material and methods

2.1. Material and specimen preparation

Rapidly solidified (plasma atomized), pre-alloyed powder of (TC4) (Arcam, Sweden) was used as a feedstock material in this work. Fig. 1(a) shows the powder morphology and size distribution, which is illustrated quantitatively in the histogram of Fig. 1(b). As shown in Fig. 1(b), the average powder size is 68 µm (d_{10}=45 µm, d_{50}=62 µm, d_{90}=85 µm). The fabrication of Cubic samples with dimensions of 20×20×5 mm^3 was performed using an Arcam A2X system (GE Additive, Arcam Sweden) operating under a vacuum atmosphere. The layer thickness was fixed at 50 µm. The samples were printed with the standard predefined EBM process parameters recommended by Arcam to minimize the final porosity in the samples.

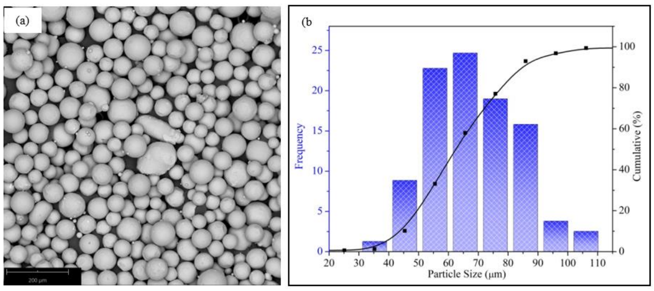

Fig 1. Powder morphology and size distribution of pre-alloyed Ti6Al4V.

2.2. Surface post-treatment

To enhance the surface quality of the EBM manufactured specimens, three different post-processing methods, including surface grinding (G), drag finishing (DF), and surface mechanical treatment (SMT), are used in this work. First of all, for grinding treatment, the surface of the as-built (AB) samples was ground with SiC grinding paper down to a 1200 grit finish. Thereafter, for the drag finishing operation, the as-built samples were treated at 220 rpm rotation for 3 hours using ceramic abrasive media with a cylindrical shape.

For SMT, The surface of the specimen was shot peened for 20 min using a similar set-up proposed by Naito et al. [30]. In summary, the recirculation shot peening as a mechanical surface treatment utilizes balls (typically 1-8 mm diameter) made of stainless steel or ceramic that repeatedly impact the surface of the specimen in random directions. During the process, the shots are accelerated by a water jet with an injection pressure of 10 MPa. The strong impact input work hardening and compressive stress to the top surface of the workpiece. Hence, In this study, 250 ceramic shots with a smooth surface finish of 0.04 µm (*Ra*), 5 mm diameter and hardness of 1100 $HV_{0.1}$ were used for the surface treatment.

2.3. Material characterization

After different post-processings, the surface region of the AB and treated specimens were analyzed using a scanning electron microscope (SEM), and X-ray diffractometer (XRD).

SEM observations were carried out using an SEM (JEOL, Japan) operated at an accelerating voltage of 20 keV. The X-ray diffraction (XRD) analysis in the as-built state and after surface treatment was performed using a Philips X'pert MPD X-ray (Philips, Netherlands) diffractometer with the CuKα1 radiation at 40 kV and 30 mA and at 2θ range of 20 to 80°. The lattice micro-strains and crystallites size in the near-surface layer were estimated based on the changes in the physical width of the diffraction peaks and achieved by employing Williamson–Hall (W–H) method.

The surface roughness of the treated surfaces was determined three times at different locations on each specimen using a MarSurf RTP80 tester according to ISO 428/JIS 80601 standard. The surface roughness was measured at a transverse speed of 0.5 mm/s. The microhardness of the specimen was measured with a Vickers indenter load of 0.1 kg.f ($HV_{0.1}$) and a dwell time of 10 s. Three measurements were carried out in different places of the treated zones for each case, and the average magnitude was reported. A contact angle goniometer was used to assess the water contact angles and surface tension using double distilled water. Five measurements were taken and averaged after depositing a droplet of water on the sample surface for 10 s under ambient circumstances. From contact angle data, the surface energy '*Es*' was calculated [31].

3. Results and discussions

3.1. Surface Morphology

To study the effect of post-treatments on the AB samples, microscopy observations were performed on the surface of the samples. Fig. 2 compares the surface morphologies of the samples after different surface post-treatments with the AB sample.

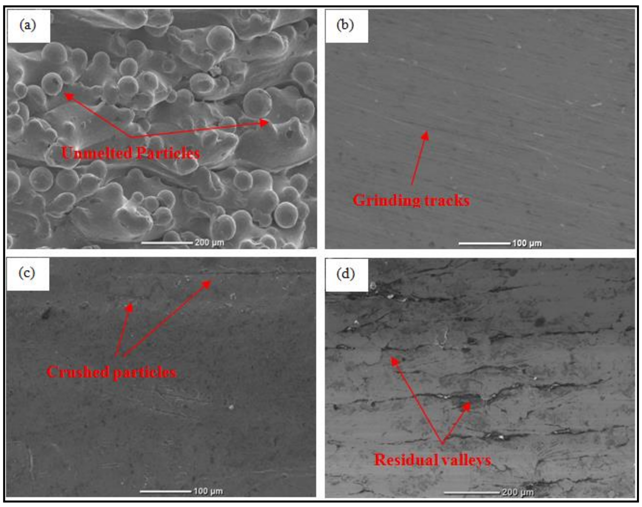

Fig. 2. SEM micrograph showing the top surface morphology of all samples, (a) AB; (b) G; (c) DF; (d) SMT.

As shown in Fig 2 (a), many partially melted particles and ripples in the molten tracks can be seen on the surface of the AB sample. As mentioned in previous reports, the surface of the AB sample has several regions that are ideal sites for crack initiation and low fatigue strength [22,32]. Fig. 2(b) and 2(c) show a surface with some scratches introduced by mechanical grinding and a relatively smooth surface with crushed metallic powders after DF, respectively. After SMT (Fig. 2(d)), the impact of the ceramic balls on the AB surface would remove some of the peaks and partially melted particles due to plastic deformation and/or fracture of materials. However, the surface valleys are still present.

3.2. Surface Roughness

The microscopic observations in Fig. 2 are confirmed by surface roughness measurements reported in Fig. 3.

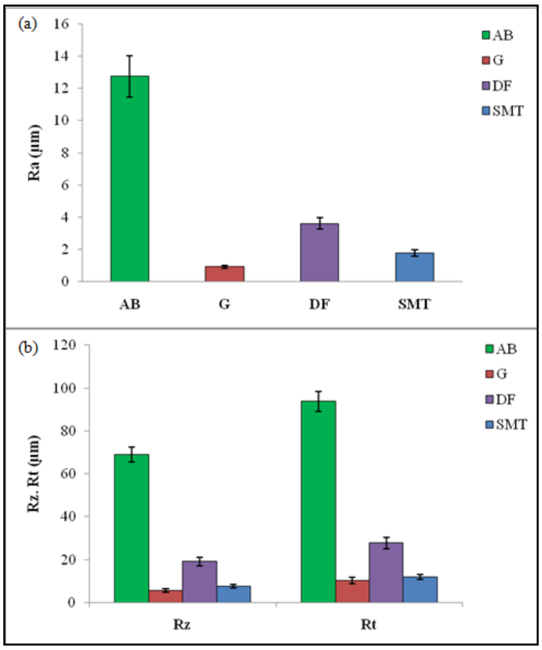

Fig. 3. Surface roughness parameters of the AB Ti6Al4V manufactured by EBM and after (G), (DF) and (SMT).

The surface roughness parameters *Ra* (arithmetic mean deviation of the assessed profile), *Rz* (maximum height of the profile) and *Rt* (total height of the profile) for the AB and treated samples are shown in Fig. 3 (a,b). The results indicate that the *Ra* and *Rz* for all post-treatment methods decreased as compared to the AB sample. Ground specimen represented the lowest surface roughness even compared to the DF series. Moreover, the surface roughness of the SMT sample is very close to the DF specimen and lower than the AB one. Indeed, in the SMT, the interaction between the surface and flying balls during the post-treatment decreased the roughness of the AB TC4 sample. The displaced materials from the deformed peaks fill the surrounding valleys and cover up some of the deep valleys. Thus, it can be concluded that a fraction of original valleys can be disappeared due to the filling or covering up by the deformed material of the peaks. This is in line with the numerous studies demonstrating the reduction of surface roughness of AM components after different mechanical post-treatment [24,27,33]. Overall, it is obvious that all these post-treatments improve the surface topography of the AM specimens.

3.3. Surface characteristics

Fig. 4 (a) compares the XRD patterns of the AB and various post-processed specimens.

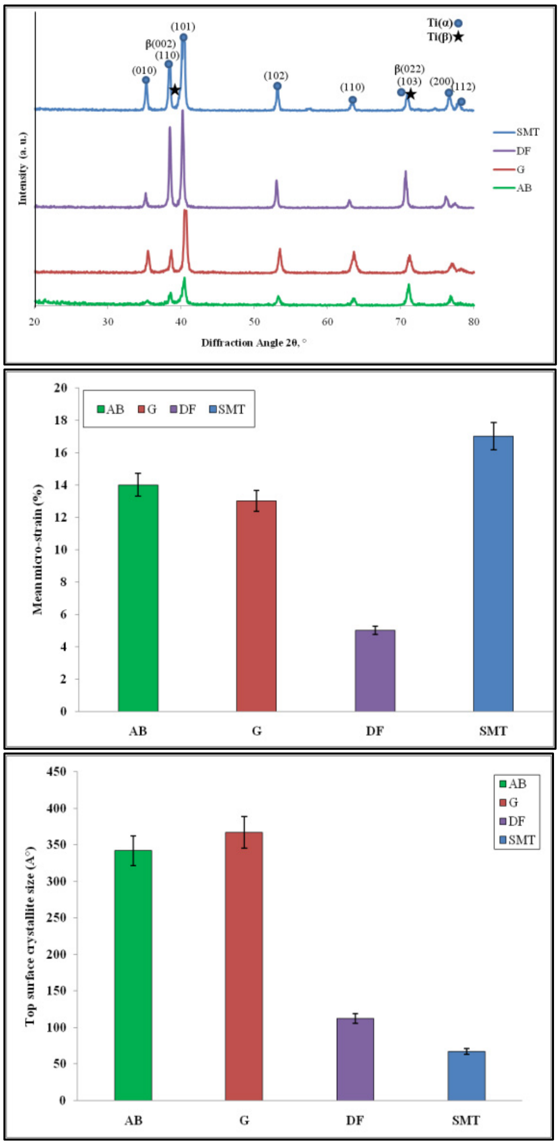

Fig. 4. a) XRD pattern of all the samples b) Top surface grain size; c) Measured micro-strain in all the specimens.

As can be seen, the dominant phase in all the specimens from the AB state to the samples after the post-treatments is alpha together with a small amount of beta–Ti. Meanwhile, the diffraction peaks of SMT samples are broader, which can be as a consequence of the refined domain sizes and increased microstrain on the surface caused by the plastic deformation.

According to XRD analyses and the Williams-Hall equation, the average crystallite size and amplitude of surface microstrain can be evaluated as presented in Fig. 4(b,c). As it demonstrated, plastic deformation induced by the SMT process caused grain refinement on the surface of the treated sample. This grain refinement produced by SMT was also previously reported by other researchers [27–29].However, no significant changes were revealed for the MP and DF samples. Indeed, the amplitude of the microstrain increases from 14% in the AB state to about 17% in the SMT sample. This may be explained by the work hardening behaviour of the material during treatment [9,28,33]. The microhardness results presented in the next section support this argument.

3.4. Hardness test

The hardness and stress state of any material are also crucial characteristics with respect to its operational life. The surface hardness values of the AB and post-processed specimens are shown in Fig. 5.

The hardness of the AB sample is about 338 HV which is in the range reported in previous works[2,19]. When the hardness of the AB sample is compared with the post-processed specimens, it is observed that the hardness of the SMT specimen was much higher than the AB and other post-treated specimens. The difference between the lowest and highest hardness is approximately 12%. According to previous results, it is obvious that the SMT operation causes strain hardening and grain refinement on the top surface of the specimens. Therefore, according to the Hall-Pitch relation, the measured hardness on the SMT surface is much larger than AB and other post-processing operations. Other researchers reported this trend that the peening treatments caused a plastic deformation and work hardening effect on both the Direct Metal Laser Sintering (DMLS) and EBM surfaces [19,34]. It is worth to be mentioned that this trend seems to be useful in terms of the wear resistance of these EBM manufactured specimens.

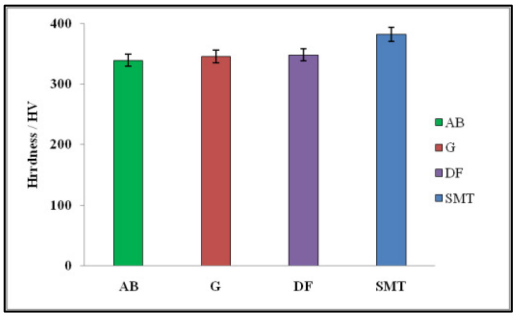

Fig. 5. Average top surface microhardness of the different samples.

3.5. Wettability

The outcomes of the surface wettability tested for measuring contact angle and surface energy by the sessile drop method with the shape of the water droplet formed on the surface of the AB and treated samples are presented in Fig. 6.

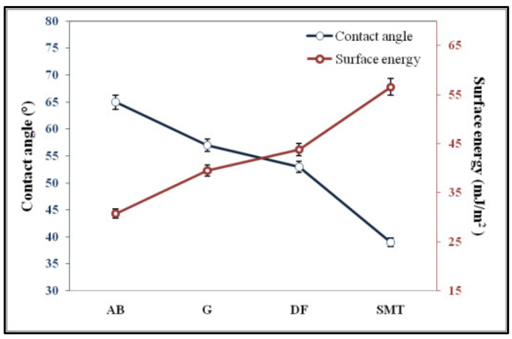

Fig. 6. Variation in contact angle and surface energy for the AB and post-treated samples.

Fig.6 clearly shows that the surface energy and wettability of the samples changed after the different surface post-treatments. Based on the XRD results, the SMT induced crystal defects on the topmost surface of materials, which results in the formation of a layer with higher surface energy, leading to enhance wettability. Hence, it should be noted that these changes to surface integrity may also directly affect the nature of the interaction between surface and surrounding environments, such as physiological solutions [35]. Previous studies have shown that increasing surface wettability can also be connected to accelerated adhesion of blood proteins, which is linked with the initial stage of the tissue healing process [36,37]. In addition, it is worth to be mentioned that surface energy is affected by surface roughness as well. So, the water angle of AB and G were different. However, these values are very close with minimal differences. Therefore, it can be stated that the SMT sample would be more suitable for the construction of long term implants produced by AM methods where strong bonding to hard tissues is required.

4. Conclusion

In this paper, the effect of different post surface treatments on the surface characteristics of TC4 samples fabricated via EBM was investigated. The main conclusions that can be drawn according to the key finding are as follow:

- The average surface roughness of G, DF, and SMT samples decreased by about 92%, 72% and 86%, respectively.
- The XRD analyses showed that SMT led to the broadening of the diffraction peaks, caused by the reduction in domain size of the alpha phase and increasing microstrain in the near-surface layers.
- Vickers microhardness results show that SMT enhances the mechanical properties of the AB samples by 11%.
- The hydrophilicity test revealed that the wettability and surface energy of the treated surfaces were more than the AB surface.

Accounting for the results obtained from surface morphology, roughness, XRD analysis, microhardness and wettability, the SMT can be recommended for the production of AM biomedical implants.

References

[1] F. Shahriyari, R. Taghiabadi, A. Razaghian, M. Mahmoudi, Effect of friction hardening on the surface mechanical properties and tribological behavior of biocompatible Ti-6Al-4V alloy, J. Manuf. Process. 31 (2018) 776–786. https://doi.org/10.1016/j.jmapro.2017.12.016.

[2] G. Del Guercio, M. Galati, A. Saboori, Innovative Approach to Evaluate the Mechanical Performance of Ti–6Al–4V Lattice Structures Produced by Electron Beam Melting Process, Met. Mater. Int. 27 (2021) 55–67. https://doi.org/10.1007/s12540-020-00745-2.

[3] L. Zhang, L. Chen, A Review on Biomedical Titanium Alloys: Recent Progress and Prospect, Adv. Eng. Mater. 21 (2019) 1801215. https://doi.org/10.1002/adem.201801215.

[4] M.H. Mosallanejad, B. Niroumand, A. Aversa, D. Manfredi, A. Saboori, Laser Powder Bed Fusion in-situ alloying of Ti-5%Cu alloy: Process-structure relationships, J. Alloys Compd. (2020) 157558. https://doi.org/https://doi.org/10.1016/j.jallcom.2020.157558.

[5] A. Saboori, D. Gallo, S. Biamino, P. Fino, M. Lombardi, An overview of additive manufacturing of titanium components by directed energy deposition: Microstructure and mechanical properties, Appl. Sci. 7 (2017). https://doi.org/10.3390/app7090883.

[6] M. Aristizabal, P. Jamshidi, A. Saboori, S.C. Cox, M.M. Attallah, Laser powder bed fusion of a Zr-alloy: Tensile properties and biocompatibility, Mater. Lett. 259 (2020) 126897. https://doi.org/10.1016/J.MATLET.2019.126897.

[7] L. Zhang, Y. Liu, S. Li, Y. Hao, Additive Manufacturing of Titanium Alloys by Electron Beam Melting: A Review, Adv. Eng. Mater. 20 (2018) 1700842. https://doi.org/10.1002/adem.201700842.

[8] M.H. Mosallanejad, B. Niroumand, A. Aversa, A. Saboori, In-situ alloying in laser-based additive manufacturing processes: A critical review, J. Alloys Compd. 872 (2021) 159567. https://doi.org/https://doi.org/10.1016/j.jallcom.2021.159567.

[9] M. Sato, O. Takakuwa, M. Nakai, M. Niinomi, F. Takeo, H. Soyama, Using Cavitation Peening to Improve the Fatigue Life of Titanium Alloy Ti-6Al-4V Manufactured by Electron Beam Melting, Mater. Sci. Appl. 07 (2016) 181–191. https://doi.org/10.4236/msa.2016.74018.

[10] A. Saboori, A. Abdi, S.A. Fatemi, G. Marchese, S. Biamino, H. Mirzadeh, Hot deformation behavior and flow stress modeling of Ti–6Al–4V alloy produced via electron beam melting additive manufacturing technology in single β-phase field, Mater. Sci. Eng. A. 792 (2020) 139822. https://doi.org/https://doi.org/10.1016/j.msea.2020.139822.

[11] M. Dadkhah, M.H. Mosallanejad, L. Iuliano, A. Saboori, A Comprehensive Overview on the Latest Progress in the Additive Manufacturing of Metal Matrix Composites: Potential, Challenges, and Feasible Solutions, Acta Metall. Sin. (English Lett. 34 (2021) 1173–1200. https://doi.org/10.1007/s40195-021-01249-7.

[12] G. Del Guercio, M. Galati, A. Saboori, Electron beam melting of Ti-6Al-4V lattice structures: correlation between post heat treatment and mechanical properties, Int. J. Adv. Manuf. Technol. 116 (2021) 3535–3547. https://doi.org/10.1007/s00170-021-07619-w.

[13] M. Galati, S. Defanti, A. Saboori, G. Rizza, E. Tognoli, N. Vincenzi, A. Gatto, L. Iuliano, An investigation on the processing conditions of Ti-6Al-2Sn-4Zr-2Mo by electron beam powder bed fusion: Microstructure, defect distribution, mechanical properties and dimensional accuracy, Addit. Manuf. 50 (2022) 102564. https://doi.org/https://doi.org/10.1016/j.addma.2021.102564.

[14] A. Saboori, S. Tusacciu, M. Busatto, M. Lai, S. Biamino, P. Fino, M. Lombardi, Production of Single Tracks of Ti-6Al-4V by Directed Energy Deposition to Determine the Layer Thickness for Multilayer Deposition, J. Vis. Exp. (2018). https://doi.org/10.3791/56966.

[15] L.E. Murr, S.M. Gaytan, D.A. Ramirez, E. Martinez, J. Hernandez, K.N. Amato, P.W. Shindo, F.R. Medina, R.B. Wicker, Metal Fabrication by Additive Manufacturing Using Laser and Electron Beam Melting Technologies, J. Mater. Sci. Technol. 28 (2012) 1–14. https://doi.org/10.1016/S1005-0302(12)60016-4.

[16] G. Del Guercio, M. Galati, A. Saboori, P. Fino, L. Iuliano, Microstructure and Mechanical Performance of Ti–6Al–4V Lattice Structures Manufactured via Electron Beam Melting (EBM): A Review, Acta Metall. Sin. (English Lett. 33 (2020) 183–203.

https://doi.org/10.1007/s40195-020-00998-1.

[17] P. Tyagi, T. Goulet, C. Riso, R. Stephenson, N. Chuenprateep, J. Schlitzer, C. Benton, F. Garcia-Moreno, Reducing the roughness of internal surface of an additive manufacturing produced 316 steel component by chempolishing and electropolishing, Addit. Manuf. 25 (2019) 32–38. https://doi.org/10.1016/j.addma.2018.11.001.

[18] E. Maleki, S. Bagherifard, M. Bandini, M. Guagliano, Surface post-treatments for metal additive manufacturing: Progress, challenges, and opportunities, Addit. Manuf. 37 (2021) 101619. https://doi.org/10.1016/J.ADDMA.2020.101619.

[19] H. Soyama, F. Takeo, Effect of Various Peening Methods on the Fatigue Properties of Titanium Alloy Ti6Al4V Manufactured by Direct Metal Laser Sintering and Electron Beam Melting, Materials (Basel). 13 (2020) 2216. https://doi.org/10.3390/ma13102216.

[20] Post-Processing of AM and 3D-Printed Parts (ISBN 978-0-9913332-8-8), 2021, https://wohlersassociates.com/post-processing-report.htm., (n.d.).

[21] J. Zhang, Y.J. Lee, H. Wang, A Brief Review on the Enhancement of Surface Finish for Metal Additive Manufacturing, 2021.

[22] H. Soyama, metals Comparison between Shot Peening, Cavitation Peening, and Laser Peening by Observation of Crack Initiation and Crack Growth in Stainless Steel, (n.d.). https://doi.org/10.3390/met10010063.

[23] S. Bagehorn, J. Wehr, H.J. Maier, Application of mechanical surface finishing processes for roughness reduction and fatigue improvement of additively manufactured Ti-6Al-4V parts, Int. J. Fatigue. 102 (2017) 135–142. https://doi.org/10.1016/j.ijfatigue.2017.05.008.

[24] L. Denti, E. Bassoli, A. Gatto, E. Santecchia, P. Mengucci, Fatigue life and microstructure of additive manufactured Ti6Al4V after different finishing processes, Mater. Sci. Eng. A. 755 (2019) 1–9. https://doi.org/10.1016/j.msea.2019.03.119.

[25] M. Zhang, C. Liu, X. Shi, X. Chen, C. Chen, J. Zuo, J. Lu, S. Ma, Residual Stress, Defects and Grain Morphology of Ti-6Al-4V Alloy Produced by Ultrasonic Impact Treatment Assisted Selective Laser Melting, Appl. Sci. 6 (2016) 304. https://doi.org/10.3390/app6110304.

[26] M. Kahlin, H. Ansell, D. Basu, A. Kerwin, L. Newton, B. Smith, J.J. Moverare, Improved fatigue strength of additively manufactured Ti6Al4V by surface post processing, Int. J. Fatigue. 134 (2020) 105497. https://doi.org/10.1016/j.ijfatigue.2020.105497.

[27] Y. Eyzat, M. Chemkhi, Q. Portella, J. Gardan, J. Remond, D. Retraint, Characterization and Mechanical Properties of As-Built SLM Ti-6Al-4V subjected to surface mechanical post-treatment, Procedia CIRP. 81 (2019) 1225–1229. https://doi.org/10.1016/j.procir.2019.03.298.

[28] Q. Zhang, B. Duan, Z. Zhang, J. Wang, C. Si, Effect of ultrasonic shot peening on microstructure evolution and corrosion resistance of selective laser melted Ti–6Al–4V alloy, J. Mater. Res. Technol. 11 (2021) 1090–1099. https://doi.org/10.1016/j.jmrt.2021.01.091.

[29] T. Persenot, A. Burr, E. Plancher, J.-Y. Buffière, R. Dendievel, G. Martin, Effect of ultrasonic shot peening on the surface defects of thin struts built by electron beam melting: Consequences on fatigue resistance, Addit. Manuf. 28 (2019) 821–830. https://doi.org/10.1016/j.addma.2019.06.014.

[30] A. Naito, O. Takakuwa, H. Soyama, Materials Science and Technology Development of peening technique using recirculating shot accelerated by water jet Development of peening technique using recirculating shot accelerated by water jet, (n.d.). https://doi.org/10.1179/1743284711Y.0000000027.

[31] D. Khang, J. Lu, C. Yao, K.M. Haberstroh, T.J. Webster, The role of nanometer and sub-micron surface features on vascular and bone cell adhesion on titanium, Biomaterials. 29 (2008) 970–983. https://doi.org/10.1016/j.biomaterials.2007.11.009.

[32] H. Soyama, Comparison between the improvements made to the fatigue strength of stainless steel by cavitation peening, water jet peening, shot peening and laser peening, J. Mater. Process. Technol. 269 (2019) 65–78. https://doi.org/10.1016/J.JMATPROTEC.2019.01.030.

[33] L. Xie, Y. Wen, L. Wang, C. Jiang, V. Ji, Characterization on Surface Properties of Ti–6Al–4V After Multiple Shot Peening Treatments, J. Eng. Mater. Technol. 138 (2016). https://doi.org/10.1115/1.4033577.

[34] W. Guo, R. Sun, B. Song, Y. Zhu, F. Li, Z. Che, B. Li, C. Guo, L. Liu, P. Peng, Laser shock peening of laser additive manufactured Ti6Al4V titanium alloy, Surf. Coatings Technol. 349 (2018) 503–510. https://doi.org/10.1016/j.surfcoat.2018.06.020.

[35] B. Boyan, Role of material surfaces in regulating bone and cartilage cell response, Biomaterials. 17 (1996) 137–146. https://doi.org/10.1016/0142-9612(96)85758-9.

[36] L.-C. Xu, C.A. Siedlecki, Effects of surface wettability and contact time on protein adhesion to biomaterial surfaces, Biomaterials. 28 (2007) 3273–3283. https://doi.org/10.1016/j.biomaterials.2007.03.032.

[37] J.I. Rosales-Leal, M.A. Rodríguez-Valverde, G. Mazzaglia, P.J. Ramón-Torregrosa, L. Díaz-Rodríguez, O. García-Martínez, M. Vallecillo-Capilla, C. Ruiz, M.A. Cabrerizo-Vílchez, Effect of roughness, wettability and morphology of engineered titanium surfaces on osteoblast-like cell adhesion, Colloids Surfaces A Physicochem. Eng. Asp. 365 (2010) 222–229. https://doi.org/10.1016/j.colsurfa.2009.12.017.